NATIONAL AERONAUTICS AND SPACE ADMINISTRATION

Technical Report 32-1546

Liquid-Phase Mixing of Bipropellant Doublets

F. W. Hoehn
J. H. Rupe
J. G. Sotter

JET PROPULSION LABORATORY
CALIFORNIA INSTITUTE OF TECHNOLOGY
PASADENA, CALIFORNIA

February 15, 1972

NATIONAL AERONAUTICS AND SPACE ADMINISTRATION

Technical Report 32-1546

Liquid-Phase Mixing of Bipropellant Doublets

F. W. Hoehn
J. H. Rupe
J. G. Sotter

JET PROPULSION LABORATORY
CALIFORNIA INSTITUTE OF TECHNOLOGY
PASADENA, CALIFORNIA

February 15, 1972

Prepared Under Contract No. NAS 7-100
National Aeronautics and Space Administration

Preface

The work described in this report was performed by the Propulsion Division of the Jet Propulsion Laboratory.

Acknowledgment

The authors wish to acknowledge the contributions of F. G. Gerbracht and J. M. Garcia for their efforts in conducting the cold flow experiments and to thank P. J. Breckheimer for his contribution in writing the computer data reduction program.

Contents

Tables

Contents (contd)

Figures

Abstract

Comparisons of cold-flow mixing efficiency for sprays formed by unlike impinging doublet injector elements comprising circular and noncircular orifices have recently been reported by other investigators. It was concluded by them that noncircular elements produce significantly better mixing efficiencies η_m than a circular unlike doublet at equivalent design conditions. The fact that the η_m value for their circular-orifice unlike doublet was significantly lower than typical values produced by other investigators for a number of other circular-orifice doublets suggested that factors other than orifice shape might have been present in the comparison.

Experimental results of unlike doublet mixing obtained at the Jet Propulsion Laboratory are correlated herein with an analytically derived equation predicting fluid cavitation. The correlation relates the minimum orifice pressure drop required to initiate cavitation, with the system back pressure, cold flow simulant vapor pressure, and the orifice flow discharge and contraction coefficients. Stream flow instabilities are also visually correlated with the onset of cavitation and orifice discharge coefficient measurements. In addition, the influence of cavitation on the characteristic phenomenon of hydraulic flip is observed for both circular and noncircular shaped orifices. For certain intermediate orifice lengths, some noncircular shapes are shown to produce more fully developed flows (shorter recovery lengths) and therefore a more cohesive jet, which in turn yields slightly higher cold flow mixing uniformities than circular shaped orifices of equal absolute length. The particular noncircular shaped elements evaluated, however, are shown to be more sensitive to liquid stream misimpingement than the corresponding circular orifices.

Liquid-Phase Mixing of Bipropellant Doublets

I. Introduction

Most liquid bipropellant rocket injectors built in the United States have spray elements incorporating the impingement of two or more liquid jets. The impingement process, properly controlled, aids in spatial distribution as well as atomization of the liquids. By using unlike (fuel-oxidizer) impingement, one can also accomplish a macroscopic mixing of the propellants within the individual element's spray pattern. The present work is concerned with the relative cold flow mixing characteristics of nonreactive liquid streams injected from orifices of circular and noncircular shapes.

Conventionally, orifices used for forming jets are circular in cross section; in the past, twist drilling has been the only economical means of machining the large number of orifices called for in most rocket injector designs.

More recent techniques, notably electrical-discharge machining (EDM), have made it practical to consider the use of noncircular orifices. The motivation for considering such orifices comes from the continuing need to maximize combustion performance of liquid propellant engines, since improvements might conceivably be realized if the old restriction on orifice shape were removed. New methods of fabricating injectors are also made practical when noncircular orifices are permissible.

The degree of macroscopic mixing can be characterized by a mixing efficiency η_m defined by Rupe (Ref. 1). It is a measure of the mixing on a macroscopic level as determined experimentally by a finite number of sampling tubes distributed on a spherical surface intercepting the spray.

As defined, this spray criterion may have any numerical value from 0 to 100 and represents all local values of mixture ratio compared to the total injected simulant mixture ratio. When η_m is 100, the mixture is everywhere uniform, at least at the macroscopic level, and when η_m is 0, the propellants are totally unmixed.

Values of η_m measured in nonreactive systems with fully developed flows from circular jets are in the range of 50–85% (Refs. 1,2). Rupe typically found maximum values between 75 and 85 near optimum conditions, and some were above this level. Rupe concluded that within limits (±5%) the mixing factor for a given circular orifice combination reaches a maximum when a correlating parameter

ϕ, the product of the ratios of the velocity heads and stream diameters, is equal to unity. This relationship, reproduced from Ref. 2, is shown in Fig. 1, for several orifice area ratios.

The mixing characteristics of other orifice configurations have been investigated recently by Nurick and McHale (Ref. 3), who used several unlike doublets having various orifice shapes but with the respective cross-sectional areas of the fuel and oxidizer orifices held constant. Noncircular orifices were designed in such a way that the facing width of the orifices in any one doublet element were equal. Nurick and McHale found in their experiments that the highest η_m for noncircular elements was 84.9, obtained with an element comprising a rectangular and a triangular orifice which they compared with an η_m of only 70.2 for a circular orifice configuration having the same orifice length, 1.52 cm (0.60 in.), even though the highest single-point mixing factor attained during their investigation was 87.0 for the circular element when its length was reduced to 0.76 cm (0.30 in.).

In single-element injector hot firings, using a hypergolic propellant combination, Nurick and McHale found that under most conditions, the characteristic velocity efficiency was higher for the rectangular-orifice doublet than for the circular orifice configuration. However, they point out that the results were not necessarily predictable from cold-flow measurements because blow-apart of the streams apparently occurred in the hot firings, resulting in observed values between 55 and 85%: combustion efficiencies considerably lower than the current state of the art.[1]

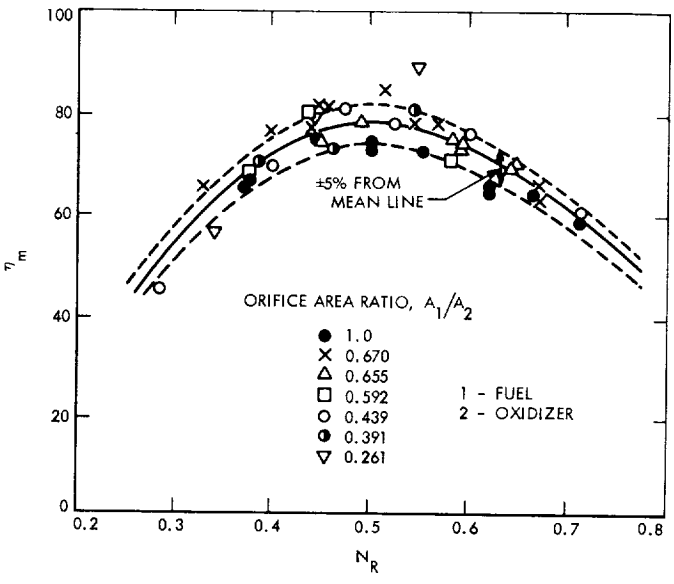

Fig. 1. Correlation of the dynamic characteristics of free liquid circular jets and mixing (Ref. 2)

On the basis of their cold flow results, Nurick and McHale ultimately concluded that "Noncircular elements produce significantly better mixing than a circular doublet at equivalent design conditions." They reached this conclusion even though the highest cold-flow mixing efficiency that they measured over a range of mixture ratios using circular orifices, 70.2, was significantly lower than optimum values previously reported by Rupe (Fig. 1), as well as the single-point maximum noted above.

Rupe's criterion has been used successfully by rocket engine manufacturers to optimize circular orifice injector designs, and for this application he emphasizes that the impinging free streams must be dynamically similar (fully developed turbulence is preferred), symmetrical, and stable. Generally, these jet characteristics are not to be expected from the orifices utilized by Nurick and McHale; hence the comparison in mixing efficiencies for impinging streams formed by various shaped orifices is questionable.

In order to verify this observation experimentally, a brief study of jet properties and the concomitant spray mixing efficiencies produced by orifice geometries identical to those used by Nurick and McHale (as well as certain additional configurations) was initiated. The present investigation was conducted at the Jet Propulsion Laboratory (JPL) with three primary objectives:

(1) To provide an independent check on the results and conclusions reached by Nurick and McHale in their nonreactive mixing study,

(2) To compare the sensitivity of bipropellant mixing to stream misimpingement for noncircular and circular doublet elements, and

(3) To extend the basic knowledge on the effects of impinging stream hydraulics and stability on liquid phase mixing.

II. Apparatus

The orifice configurations included various combinations of circular, rectangular, and triangular shaped holes previously tested by Nurick and McHale. The diameter of the

[1]Under conditions in which gaseous reaction products are generated rapidly at the interface between the fuel and oxidizer jets, mixing characteristics are modified. The phenomenon, termed "blow-apart," has been investigated by Johnson (Ref. 4), Houseman (Ref. 5), and others, and generally results in reduced performance of single-element injectors.

circular orifice for the oxidizer system was 0.182 cm (0.0718 in.) and the corresponding fuel diameter hole was 0.160 cm (0.0631 in.). The noncircular shapes were designed with equivalent respective flow areas. Additional element pairs of the same basic configuration were made by selecting shapes with different orifice height/width ratios. Due to manufacturing tolerances, this change incidentally affected the fuel-to-oxidizer element area ratios somewhat. All orifices were initially machined with sharp edges into interchangeable inserts 1.52 cm (0.60 in.) thick, resulting in a range of length to hydraulic diameter (L/D_h) ratios from 8.6 to 13.3. Subsequent cold flow mixing tests made with variable manifold cross velocities utilized these same orifice inserts after modification by machining to a thickness of 0.76 cm (0.30 in.).[2] The results previously obtained with these orifices are given in Ref. 3 and will be used as required in the comparisons reported herein.

The JPL orifice test hardware (Table 1) consisted of long (L/D = 100) circular elements designated configuration STD, a circular orifice element ($L/D \sim 9$) with both sharp (configuration A) and contoured (configuration A-RND) entrances, a rectangular element designated configuration

[2]These orifices, together with the cold flow test hardware, were supplied by Rocketdyne, A Division of North American Rockwell Corporation, through the cooperation of the National Aeronautics and Space Administration.

Table 1. Summary of JPL unlike doublet element designs

Element type	Element Shape[a] cm (in.) Oxid	Element Shape[a] cm (in.) Fuel	Hydraulic diameter cm (in.) Oxid	Hydraulic diameter cm (in.) Fuel	L/D_h Oxid	L/D_h Fuel	Orifice area cm^2 ($in.^2$) Oxid	Orifice area cm^2 ($in.^2$) Fuel	Area ratio Fuel/oxid
STD			0.185 (0.0730)	0.185 (0.0730)	100	100	0.0269 (0.00418)	0.0269 (0.00418)	1.000
STD(MOD)			0.185 (0.0730)	0.083 (0.0330)	100	100	0.0269 (0.00418)	0.0054 (0.00085)	0.204
A			0.179 (0.0706)	0.159 (0.0628)	8.5	9.6	0.0252 (0.00391)	0.0199 (0.00309)	0.792
A-RND			0.179 (0.0706)	0.159 (0.0628)	8.5	9.6	0.0252 (0.00391)	0.0199 (0.00309)	0.792
D	0.093 × 0.259 (0.0368 × 0.102)	0.092 × 0.190 (0.0365 × 0.075)	0.137 (0.0541)	0.124 (0.0491)	11.1	12.2	0.0241 (0.00375)	0.0176 (0.00274)	0.731
D(MOD)	0.095 × 0.249 (0.0375 × 0.0983)	0.090 × 0.182 (0.0356 × 0.072)	0.138 (0.0543)	0.120 (0.0476)	27.6	31.5	0.0238 (0.00369)	0.0165 (0.00256)	0.694
W	0.114 × 0.259 (0.0451 × 0.102)	0.092 × 0.190 (0.0365 × 0.075)	0.158 (0.0625)	0.124 (0.0491)	24.0	30.5	0.0296 (0.00460)	0.0176 (0.00274)	0.595

[a] Concentric symbol denotes rounded entrance.

D ($L/D_h \sim 12$), a rectangular orifice designated D(MOD) (contoured inlet with $L/D_h \sim 30$), and a modified rectangular shape W with unequal orifice widths ($L/D_h \sim 27$). Whenever it was necessary to duplicate Nurick and McHale's original configurations for orifices that had been modified, new orifice inserts that were identical (within reasonable manufacturing tolerances) to the original inserts were fabricated at JPL from the original drawings. Each pair of individual orifice inserts formed a single unlike doublet element with a 1.047-rad (60-deg) included angle when installed in the cold flow injector fixture.

Supplementary examination of the effects of impingement angle and alignment on mixing efficiency was accomplished in a JPL-designed fixture (Fig. 2). This apparatus was designed to optimize the axial symmetry and reproducibility of the hydraulic properties for the individual streams. The dimensions and alignment of the orifices were determined by the JPL Inspection Department prior to each cold flow test series. Each unlike doublet element was aligned to within 0.0254 mm (0.001 in.) centerline displacement.

III. Experimental Procedures

The JPL techniques used for evaluating sprays have been previously reported (Ref. 1). Basically, the test fixture was mounted in a spray-test facility and the simulants flowed vertically downward through ambient air toward a collection device. The collection apparatus employed was the same one used previously by Rupe and Gerbracht (Ref. 6). A photograph of the collection apparatus is shown in Fig. 3.

The nonreacting liquids used to simulate liquid propellants were trichloroethylene (oxidizer) and water (fuel). The density ratio of this liquid combination approximates that of nitrogen tetroxide and hydrazine, respectively, although the present investigation was conducted without reference to any specific propellant combination.

Briefly, the JPL experimental technique involved obtaining samples of the spray at an array of angular locations covering the spray. This was accomplished by rotating the collector on its axis in increments of 0.261 rad (15 deg) and photographically recording and emptying the collector tube contents between successive angular positions. The injector was positioned with the stream impingement point located on the collector axis at a radius of 15.24 cm (6.0 in.) from the spherical collection surface.

For comparison, the collection surface used by Nurick and McHale was planar, containing a 32 by 32-tube matrix.

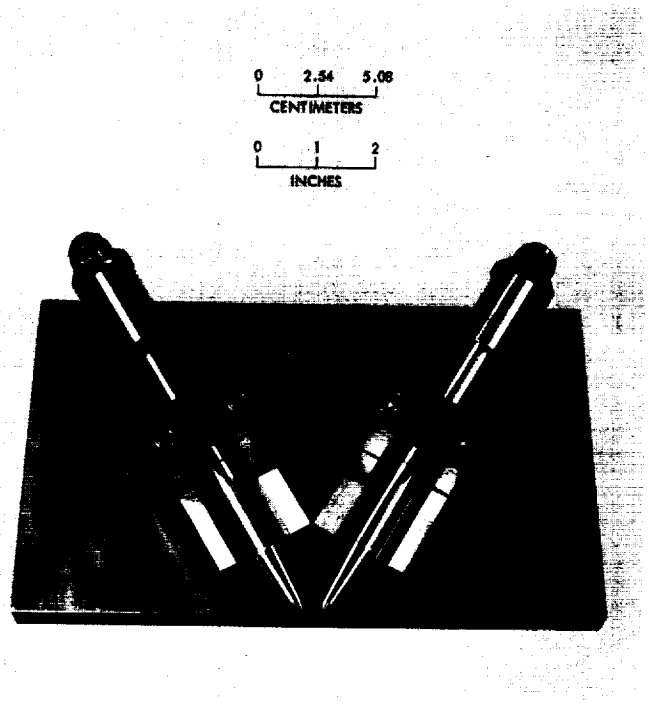

Fig. 2. Orifice alignment fixture (Ref. 6)

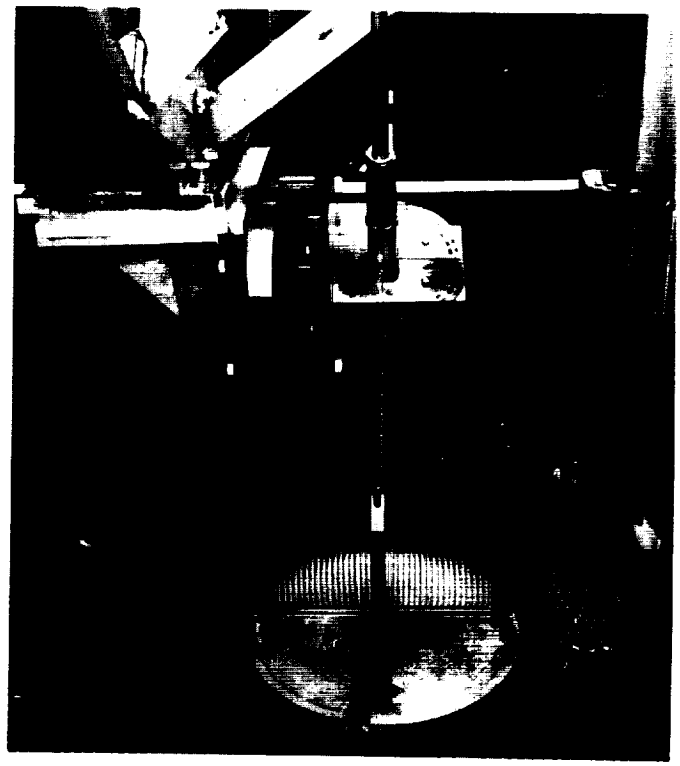

Fig. 3. Experimental apparatus in test configuration (Ref. 6)

All tests were conducted with the injector element centered above the collector at a distance of approximately 7.62 cm (3 in.). The individual simulant volumes were determined by emptying the contents of the collector tubes into a graduated cylinder. None of the results reported herein appear to be significantly influenced in any way by these differences in apparatus and experimental technique.

Since immiscible fluids were used by both agencies as propellant simulants for bipropellant elements, it was possible to obtain both a total mass and a ratio of the masses of the two fluids for each sample location. Thus, the mass and mixture ratio spatial distributions as well as the η_m for the spray could be determined. The mixing factor η_m for the JPL data was calculated by the following expression:

$$\eta_m = 100\left[1 - \left(\sum_0^n \frac{Cw(R-r)}{WR} + \sum_0^{\bar{n}} \frac{C\bar{w}(R-\bar{r})}{W(R-1)}\right)\right]. \quad (1)$$

This mixing factor, first defined by Rupe (Ref. 1), is based upon the statistical variations in the local (collected) propellant mass fractions compared to the overall injected condition. The fractional parts collected are mass-weighted according to the total *injected* flow. The η_m is generally correlated with a parameter N_R which is defined by the following expression:

$$N_R = \frac{1}{1+\phi} = \frac{1}{1 + \dfrac{\rho_1 V_1^2 D_1}{\rho_2 V_2^2 D_2}} . \quad (2)$$

A collector efficiency η_c was also calculated for each test. This is a measure or an accounting of the total injected flow W vs the collected flow

$$\eta_c = \frac{\sum_0^n Cw + \sum_0^{\bar{n}} C\bar{w}.}{W} \quad (3)$$

The collector efficiency was calculated by dividing the summations represented by the individual collector tube liquid volumes by the input flow (measured with turbine flowmeters during a precise time interval).

Collector efficiencies of 85–90% were typically obtained by Rupe in his early experiments where the resultant momentum vector of the spray was always adjusted to coincide with the axis of the collector. However, for the results reported herein, the momentum vector was allowed to change with operating conditions (also a characteristic of the procedures used by Nurick and McHale) and it was observed that there was a concomitant variation in η_c. In order to minimize this effect in the *comparisons* presented herein, a modified mixing factor was computed. The reference value for the mass weighting factor was arbitrarily modified to yield a collector efficiency of 90%. The effect on η_m was never large (in the range of 2–4%) but the correction appears justified on the basis of achieving consistency in the reported results.

Data reduction and mass distribution plotting were accomplished directly by computers for both agencies. The square collector data was programmed to generate plots using a cartesian coordinate system. The JPL experimental technique provided results amenable to machine plotting using polar coordinates. Examples of selected mass distributions are presented in a later section of this report.

IV. Experimental Results and Discussion

In addition to an independent analysis of the results from Nurick and McHale's cold flow mixing tests (Ref.3), JPL conducted 22 tests to: (1) check out the apparatus and experimental methods, (2) substantiate the previous results obtained on similar injector configurations, (3) investigate the sensitivity of bipropellant stream mixing to orifice dimensions and alignment, and (4) extend the basic knowledge of the stability and stream mixing characteristics of liquid jets over a range of design parameters and operating conditions. A summary of the tests conducted by JPL is given in Table 2. Results from the JPL and previous programs are summarized in Tables 3 and 4, respectively.

A. Checkout of Apparatus and Experimental Methods

The first two JPL runs were made using a pair of equal-diameter circular orifices and was a repeat of tests previously reported by Gerbracht (Ref. 6). The contoured orifices were both 1.85 mm (0.073 in.) in diameter and 100 diameters in length. The purpose of these tests was simply to check the experimental technique by comparison with previous results. The calculated mixing factors η_m were 79.5 and 73.8 for N_R = 0.46 and 0.54 respectively. This compares satisfactorily with Gerbracht's value of 76.3, which was obtained using a mixture of perchlorethylene and kerosene and with N_R = 0.50.

Table 2. JPL program test matrix

Test No.	Type	γ, rad (deg)	Element alignment	θ, rad (deg)	δ, mm (in.)	Element Shape: Oxid	Element Shape: Fuel	Remarks
1	STD	1.047 (60)	Aligned		—[a]	See Table 1		Checkout test
2	STD	1.047 (60)						Checkout test
3	A	1.047 (60)						Verify Ref. 3 data
4	D	1.047 (60)						Verify Ref. 3 data
5	W	0.785 (45)						$X_2 > X_1$
6	W	0.785 (45)						Vary N_R
7	D(MOD)	1.047 (60)						Baseline test
8	STD (MOD)	1.047 (60)	Aligned		—[a]	See Table 1		$D_2 >> D_1$
9	STD	1.047 (60)	Centerline displaced		0.381 (0.015)	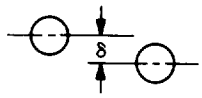		Stream misimpingement
10	D(MOD)	1.047 (60)	Centerline displaced		0.381 (0.015)	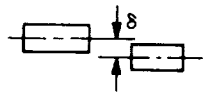		Stream misimpingement
11	D(MOD)	1.047 (60)	Angular misalignment	0.785 (45)		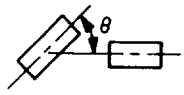		Stream misimpingement
12	D(MOD)	1.047 (60)	Angular misalignment	1.570 (90)		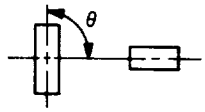		Stream misimpingement
13		1.047 (60)	Aligned misalignment			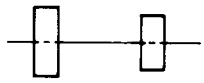		New orientation
14		1.047 (60)	Centerline displaced		0.381 (0.015)	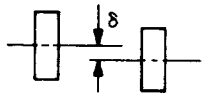		Stream misimpingement
15		0.785 (45)	Aligned			See Table 1		Vary γ
16	D(MOD)	1.308 (75)	Aligned			See Table 1		Vary γ

Table 2. (contd)

Test No.	Type	γ, rad (deg)	Element alignment	θ, rad (deg)	δ, mm (in.)	Element Shape: Oxid	Element Shape: Fuel	Remarks
17	D(MOD)	1.047 (60)	Aligned			See Table 1		Vary N_R
18	D(MOD)	1.047 (60)						
19	A-RND	1.047 (60)						
20	A-RND	1.047 (60)						
21	A-RND	1.047 (60)						
22	A-RND	1.047 (60)	Aligned			See Table 1		Vary N_R

[a] δ < 0.001-in. for aligned element.

B. Verification of Previous Results

The standard of comparison for the liquid mixing of impinging jets formed by noncircular shaped orifices was the conventional circular unlike doublet, configuration A. The JPL hole diameters were 1.79 and 1.59 mm (0.0706 and 0.0628 in.) respectively, for the oxidizer and fuel orifices.

The η_m mixing results for configuration A are plotted in Fig. 4 as a function of N_R. These data are identified with a circular symbol. All JPL data are additionally identified with a flagged marker.

The mean dashed line in Fig. 4 correlates previous data (Ref. 2) for fully developed turbulent jets for an unlike doublet element with an area ratio of 0.67. The correlation was obtained using regression analysis techniques. The standard deviation of the data about the mean curve is only ±3.3%; however, a range of ±5% is indicated to allow comparison with the recent results obtained at slightly different area ratios. The doublet area ratios for the current circular element pairs (configuration A) were 0.75 and 0.79, respectively.

Previously unpublished results (Ref. 7) are also shown for the same orifice configurations with rounded entrances (configuration A-RND) as well as sharp entry circular orifices with shorter ($L/D \sim 5$) lengths. Two data points for the latter configuration were obtained by Nurick and McHale with manifold cross velocities of 3.048 and 6.096 m/s (10 and 20 ft/s). The η_m value (87.0) for test 047, also made with the shorter length orifice, was the highest reported and suggests that the flow was entirely detached

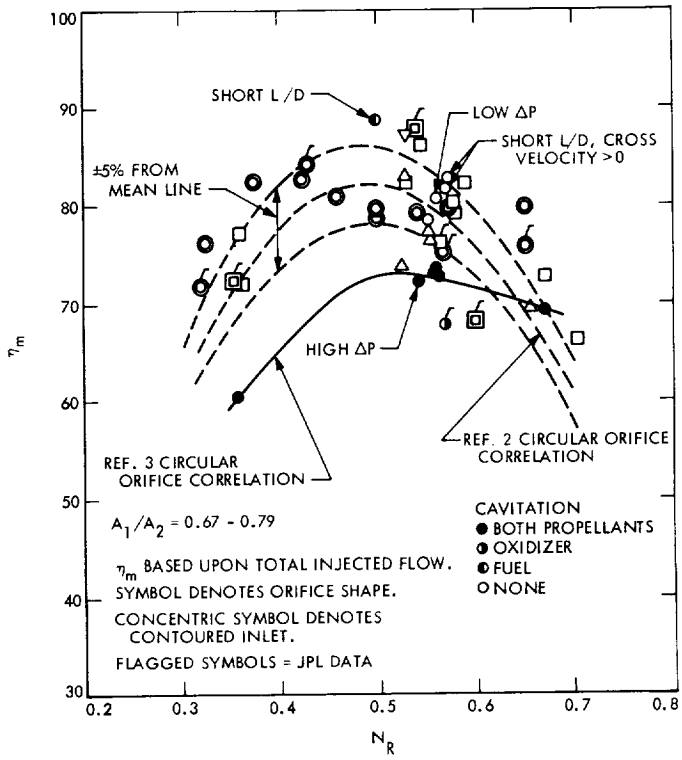

Fig. 4. Mixing results for single-element unlike doublets

Table 3. Summary of JPL results

Test	Type	C_{D_2}[a]	C_{D_1}	$1/(1+\phi)$[b]	A_1/A_2	η_m[c]	Critical[d] ΔP_2	Critical[e] ΔP_1	Oxidizer critical ratio (2)	Fuel critical ratio (1)
1	STD	0.624	0.540	0.481	1.000	79.51				
2	STD	0.617	0.523	0.542	1.000	73.78				
3	A	0.720	0.633	0.569	0.790	67.89	34.34	176.19	1.165	0.250
4	D	0.684	0.699	0.566	0.731	76.63	53.08	40.51	0.829	1.111
5	W	0.988	0.697	0.569	0.596	86.81				
6	W	0.985	0.704	0.539	0.596	68.49				
7	D(MOD)	0.841	0.757	0.540	0.694	87.76				
8	STD(MOD)	0.633	0.393	0.498	0.203	78.35				
10	D(MOD)	0.841	0.757	0.540	0.694	67.95				
11	↓	0.841	0.757	0.540	0.694	75.05				
12		0.841	0.757	0.540	0.694	69.10				
13		0.841	0.757	0.540	0.694	76.70				
14		0.841	0.757	0.540	0.694	64.46				
15		0.841	0.757	0.540	0.694	80.72				
16		0.841	0.757	0.540	0.694	83.80				
17	↓	0.875	0.769	0.355	0.694	72.22				
18	D(MOD)	0.850	0.765	0.598	0.694	68.03				
19	A-RND	0.949	0.875	0.569	0.790	75.16				
20	↓	0.908	0.950	0.320	0.790	71.93				
21	↓	0.956	0.938	0.430	0.790	84.24				
22	A-RND	0.987	0.891	0.648	0.790	75.85				

[a]Where $C_D = \dfrac{w}{A\,(2g\rho\Delta P)^{1/2}}$.

[b]Where $\phi = \dfrac{\rho_1 V_1^2 D_1}{\rho_2 V_2^2 D_2}$.

where subscripts are: 1 — fuel
2 — oxidizer

[c]With η_m calculated according to Eq. (2), where R and W are based upon injection conditions.

[d]Critical $\Delta P = \dfrac{P_B - P_V}{a^2 - 1}$ (see p. 18).

[e]Critical ratio = $\dfrac{\text{Actual } \Delta P}{\text{Critical } \Delta P}$.

from the walls.[3] Similarly, the two tests made with cross velocities yielded η_m results (79.9 and 79.7) similar to the previous Rupe (Ref. 2) data. The existence of manifold crossflow during these particular tests is believed by these authors to have introduced only secondary effects on mixing.

Four tests were also conducted at JPL with the A-RND configuration and the results are shown in Fig. 4. Mixing results for various elements comprising noncircular shaped orifices with similar orifice area ratios are also presented in this same figure. Previous data for elements with rectangular orifices (configurations C and D from Table 4) and triangular orifices (E and F from Table 4) are shown. The JPL data for rectangular orifice element D (76.6) was obtained during test 4. Also shown are three JPL results for longer ($L/D \sim 30$) rectangular orifices with contoured inlets: configuration D(MOD). The highest η_m attained was 87.7 at $N_R = 0.54$. A significant number of these η_m test results fall within or above the original ±5% band established for the Ref. 2 mixing data for fully developed circular orifice flow.

The solid line in Fig. 4 correlates a particular series of data over a range of N_R from 0.35 to 0.67. It was on the basis of these data that Nurick and McHale (Ref. 3) assigned an η_m of 70.2 as representative of the circular orifice configuration. This value, when adjusted by the appropriate mass weighting factor, becomes equal to 73.2 as shown in Fig. 4. The corresponding JPL data point (duplicating orifice geometry and flow conditions) was 67.9,

[3]Unless specified otherwise, the η_m results reported herein are the direct experimental values and are not adjusted for variations in collector efficiency.

Table 4. Summary of Nurick and McHale's results (Ref. 3)

Test	Type	C_{D_2}	C_{D_1}	$1/(1+\phi)$	A_1/A_2	η_m[a]	Critical ΔP_2	Critical ΔP_1	Oxidizer critical ratio (2)	Fuel critical ratio (1)
1	A	0.769	0.756	0.560	0.749	70.24	22.76	23.52	2.021	2.083
2	A	0.790	0.749	0.357	0.749	57.15	19.78	24.84	1.466	3.140
3	A	0.715	0.877	0.669	0.749	67.40	36.11	11.78	1.717	2.291
4	B	0.832	0.892	0.555	0.807	74.21	15.57	11.08	2.697	3.157
5	B	0.848	0.790	0.366	0.807	70.24	14.37	18.63	1.949	3.597
6	B	0.752	0.844	0.692	0.807	59.88	25.82	13.81	2.440	1.955
7	C	0.828	0.925	0.588	0.682	80.01	15.94	9.69	2.134	3.303
8	C	0.788	0.893	0.363	0.682	69.69	20.05	11.00	1.197	5.001
9	C	0.786	0.897	0.703	0.682	62.21	20.39	10.84	2.060	2.305
10	D	0.805	0.905	0.546	0.699	84.76	18.15	10.47	2.149	3.820
11	D	0.780	0.844	0.361	0.699	74.48	21.22	13.82	1.414	5.065
12	D	0.751	0.893	0.671	0.699	69.61	26.18	11.04	2.101	2.717
13	E	0.806	0.880	0.529	0.712	84.82	18.04	11.67	2.051	3.256
14	F	0.775	0.854	0.532	0.712	81.32	21.91	13.14	1.826	3.044
15	H	0.828	0.789	0.563	0.782	78.69	15.89	18.73	2.329	1.869
16	H	0.838	0.752	0.357	0.782	76.18	15.12	24.39	1.587	2.460
17	H	0.809	0.814	0.676	0.782	70.45	17.65	16.15	2.719	1.734
18	F	0.820	0.840		0.712	73.15	16.61	14.06	1.565	4.409
19	F		0.651	0.654	0.712	65.84	7.32	92.49	3.825	0.541
20	J	0.802	0.807	0.661	0.820	73.34	18.41	16.79	2.010	1.847
21	J	0.807	0.806	0.440	0.820	70.78	17.90	16.96	1.341	3.007
22	J	0.785	0.787	0.753	0.820	65.75	20.52	19.02	2.290	1.209
23	P	0.703	0.822	0.798	0.889	68.01	41.34	15.49	1.766	2.324
24	P	0.717	0.763	0.638	0.889	84.98	35.25	22.45	1.362	2.850
25	P	0.705	0.812	0.862	0.889	64.38	40.21	16.33	2.164	1.714
26	R	0.721	0.872	0.703	0.938	68.44	34.04	12.07	2.350	2.735
27	R	0.721	0.847	0.508	0.938	80.09	33.82	13.57	1.567	3.980
28	R	0.697	0.849	0.802	0.938	66.41	44.41	13.43	2.365	1.862
29	T	0.733	0.918	0.677	0.940	64.16	30.39	9.96	2.961	4.116
30	T	0.609		0.531	0.940	79.39		5.50		6.546
31	T	0.720	0.907	0.801	0.940	61.20	34.19	10.40	3.364	2.885
32	A	0.764	0.767	0.560	0.749	69.14	23.62	21.76	1.905	2.160
44	P	0.701	0.741	0.298	0.889	78.61	42.02	26.66	0.762	3.226
45	R	0.755	0.888	0.391	0.938	84.20	25.28	11.25	1.543	5.598
46	T	0.809	0.789	0.399	0.940	79.42	17.69	18.78	2.205	4.953
47	A	0.662	0.689	0.499	0.749	87.00	76.70	46.04	0.704	1.314
51	A	0.654	0.649	0.569	0.749	79.88	91.53	99.46	0.656	0.553
52	D	0.713	0.747	0.527	0.699	81.21	37.04	25.37	1.350	2.246
53	F	0.817	0.747	0.525	0.712	71.82	16.90	25.29	2.071	1.858
54	F	0.818	0.715	0.553	0.712	75.40	16.79	33.78	2.144	1.392
55	D	0.726	0.690	0.576	0.699	79.55	32.48	45.73	1.540	1.246
56	D	0.726	0.690	0.576	0.699	76.21	32.48	45.73	1.540	1.246
57	F	0.831	0.711	0.553	0.712	73.84	15.71	35.56	2.228	1.336
58	A	0.657	0.642	0.572	0.749	79.65	84.70	122.31	0.702	0.458
60	A	0.718	0.726	0.551	0.749	73.71	34.90	30.45	2.006	2.233
61	A	0.687	0.682	0.542	0.749	69.02	50.82	50.80	5.510	5.709
62	A	0.819	0.796	0.560	0.749	78.92	16.74	18.01	0.478	0.444
63	A	0.687	0.722	0.563	0.749	69.84	50.40	31.65	1.826	2.465
64	ARND	0.977	0.977	0.542	0.749	76.78				

[a] η_m calculation used R and W values based upon collector conditions.
[b] Critical ΔP ratio = measured ΔP/critical ΔP.

which represents an even greater departure from the previous results of Rupe. As discussed later in this report, these observed low η_m values are not representative of circular orifice element mixing with fully developed flow but are a result of fluid cavitation.

C. Mass and Mixture Ratio Distributions

Propellant simulant mass-flux and mixture ratio distribution contour plots were obtained on selected tests. The contour intervals selected for the contour plots in the present investigation are identified in Table 5. Mass-flux values are normalized to the maximum local mass flux. In regions of negligible mass flux, a mixture ratio of zero has been assumed arbitrarily, in order to present closed contours.

Table 5. Identification of contour values used in plots

Mass flux label	G/G_{max}
A	0.05
B	0.10
C	0.20
D	0.30
E	0.40
F	0.50
G	0.60
H	0.70
I	0.80
J	0.90
Mixture ratio label	r
A	0.1972
B	0.2998
C	0.4556
D	0.6926
E	1.0526
F	1.6000
G	2.4318
H	3.6962
I	5.6179
J	12.9781

Mass and mixture ratio plots for the sharp-edged circular element (configuration A) are presented in Fig. 5. Relatively broad spray fans are shown with the mass symmetrically distributed about the element centerline. Typical for circular impinging stream mixing, the propellant simulants are shown to penetrate through the unlike stream. The zone of highest oxidizer concentration, for example, lies opposite the oxidizer orifice.

A considerably narrower spray fan is shown in Fig. 6, resulting from the impingement of noncavitating turbulent jets. This fan was produced by the same pair of orifices,

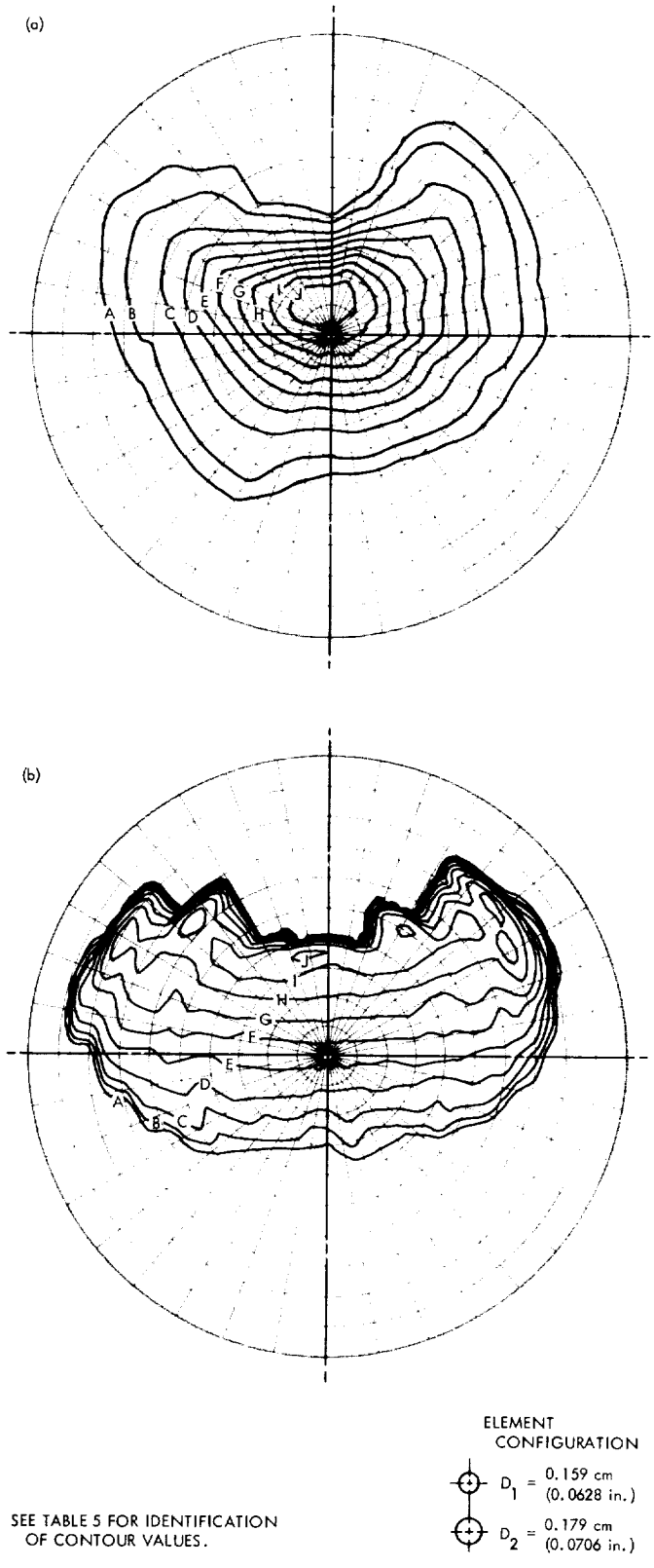

Fig. 5. Mass-flux (a) and mixture ratio (b) contours obtained from circular doublet configuration A, $L/D \sim 10$, sharp-edged entry

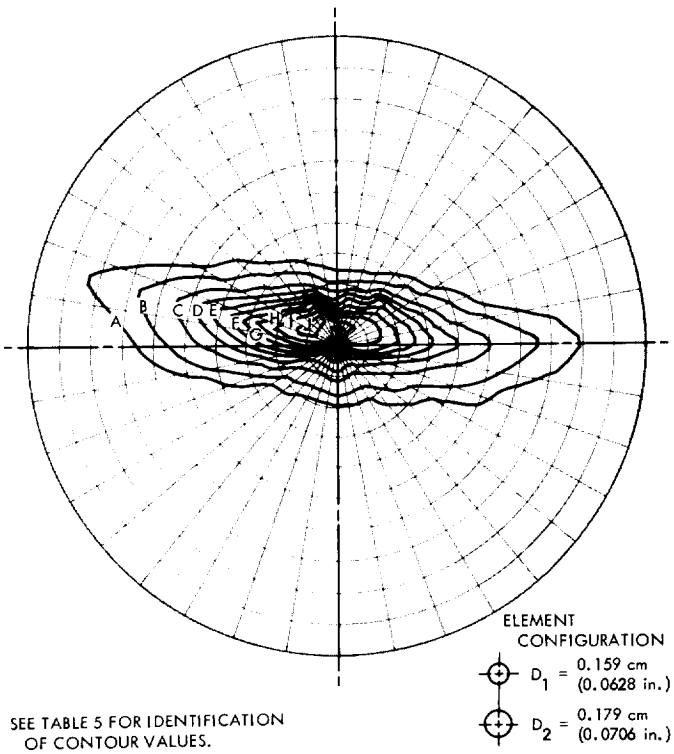

Fig. 6. Mass-flux contours obtained from circular doublet with rounded entrances, configuration A-RND, $L/D \sim 10$

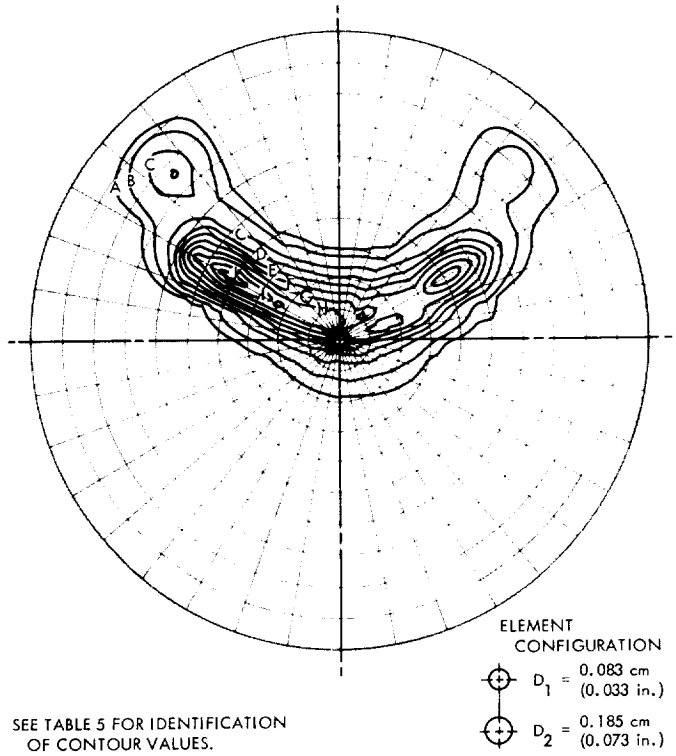

Fig. 7. Mass-flux contours obtained from circular doublet with rounded entrances, configuration STD(MOD), $L/D \sim 100$, $D_2 >> D_1$

except that they had rounded entrances (configuration A-RND). The wider fan (Fig. 5), which was indicative of impinging, brushy streams caused by fluid cavitation, is explained by the ineffectiveness of momentum interchange; i.e., impingement that is symmetrical only on a time-averaged basis.

Figure 7 shows a distorted spray fan formed by impinging circular streams injected from rounded entrance orifices with significantly different diameters.

A contour plot of total propellant mass flux for the sharp-edged rectangular element is shown in Fig. 8. The occurrence of the two side peaks is not surprising; a rectangular stream impinging at an acute angle onto a solid surface, with the minor dimension of the jet parallel to the surface, can be observed to split into two streams which go off at equal acute angles relative to the direction of the original stream.

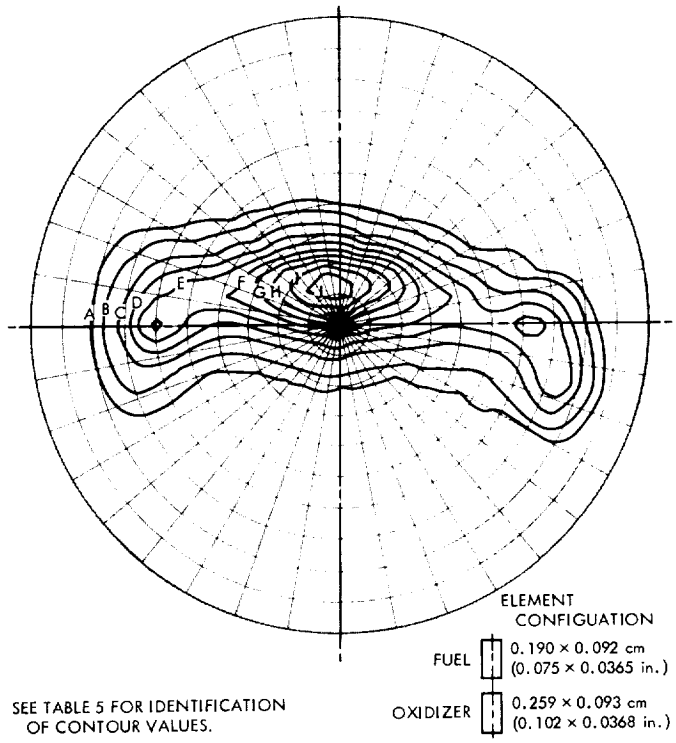

Fig. 8. Mass-flux contours obtained from rectangular doublet, configuration D, $L/D \sim 10$, sharp-edged entry

D. Design-Variable Effects

1. Orifice misalignment. Excessive manifold cross velocities, nonsymmetrical velocity profiles in the streams from

any cause, or unstable stream properties resulting from cavitation can result in uncontrolled liquid propellant mixing. Impinging, misaligned streams caused by excessive injector fabrication tolerances can also produce poor mixing efficiencies. The specification of manufacturing tolerances is more complex for injector elements utilizing noncircular shapes. In addition to lateral displacement of orifice centerlines, the possible angular rotation of either noncircular shape must also be considered. Also, for rectangular shapes, two sides must be parallel and two perpendicular in order for the centerline to adequately relate to the shape.

a. Lateral misalignment. Test 9, although originally scheduled, had previously been run by Gerbracht (Ref. 6) to study stream misimpingement and therefore was not repeated during the current investigation. In a study of the effects of manufacturing tolerances, Gerbracht found that a centerline misalignment of 0.381 mm (0.015 in.) for two equal-diameter 1.85-mm (0.073-in.) orifices produced a 14.3% degradation in the absolute value of η_m obtained for the aligned case.[4] Gerbracht used a single pair of circular orifices, each of which was 100 diameters long with rounded entrances. On a diameter percentage basis, a misalignment of 15% caused a 10% loss in η_m. These data are represented in Fig. 9. Also shown are the appropriate propellant mass distribution plots which graphically illustrate the distortion of the resulting spray fans caused by stream misimpingement. Orifice pairs were considered to be aligned during the current program if the centerline displacement was less than 0.0254 mm (0.001 in.).

Lateral displacement of the orifice centerline was investigated for the rectangular element with two different relative orifice orientations, edge-to-edge and face-to-face. Test 7 (η_m = 87.7) represented the base line edge-to-edge condition for a misimpingement and orientation study for noncavitating, rectangular shaped impinging jets. For this test the orifice centerlines were aligned and then intentionally misaligned 0.381 mm (0.015 in.) for test 10, causing a 22.5% reduction in η_m. Test 13 was made to determine the mixing characteristics of the element configured with the long sides of each rectangular orifice facing, causing the flat faces of the noncircular jets to impinge. This configuration was then tested with the orifice centerline displaced laterally 0.381 mm (0.015 in.). The misalignment produced a 15.5% η_m reduction. It is shown, therefore, that these particular noncircular orifice configurations experienced a greater reduction in mixing efficiency than the circular element for the same absolute misalignment.

[4]All quoted variations of η_m are percentages of the reference values.

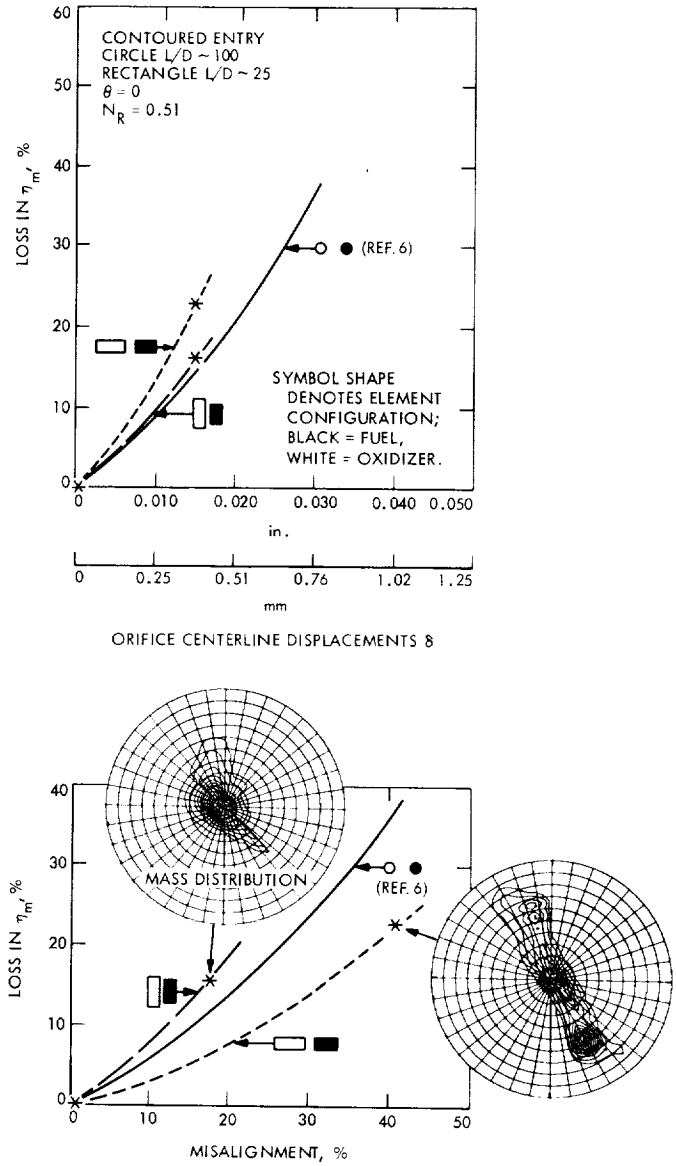

Fig. 9. Mixing efficiency influenced by orifice alignment

The results, expressed in terms of percent misalignment, are also presented in Fig. 9. The absolute displacement is expressed as a fraction of the average facing dimension for the noncircular shapes. For edge-to-edge stream impingement, a misalignment of 15% caused a 5.5% loss in η_m, while the opposite orientation produced a 13.3% loss for the same relative displacement. On a percentage basis, therefore, the rectangular element with edge-to-edge orientation demonstrated the least sensitivity to stream misimpingement.

b. Angular misalignment. Angular misalignment effects are illustrated in Fig. 10 for a particular rectangular shaped

doublet configuration. For the three-test series, the position of the fuel orifice remained constant while the orientation of the oxidizer orifice was rotated from the initial aligned position to θ = 0.785 rad (45 deg) and 1.570 rad (90 deg). By interpolation, an angular misalignment of only 0.174 rad (10 deg) corresponds to a loss of 4.5% in η_m. This type of geometrical misalignment, of course, has no physical significance for the circular unlike doublet configurations.

2. Relative orifice width. When density ratio and mixture ratio are fixed by a particular propellant combination, the diameter ratio will not in general be unity for optimum η_m (see Section I). This dimensional disparity distorts the resulting spray fan shape and could impair atomization. A possible advantage initially envisioned for the noncircular configured element, therefore, was that the concept lends itself to the design of orifices with equal widths but unequal orifice areas which do not exhibit a comparable distortion.

For circular orifices, the distorted spray fan formed by an element with significantly different orifice diameters is shown in Fig. 7. For that case (Test 8), the fuel diameter was 0.084 cm (0.033 in.) and the oxidizer diameter was 0.185 cm (0.073 in.). The mixing level was not adversely affected, however, as shown in Table 3 for long ($L/D \sim 100$) circular elements.

A condition analogous to unequal orifice widths is shown, therefore, not to degrade mixing for the circular unlike doublet element. (Nothing can be said about the effect on atomization, using only these data.)

For noncircular orifices, tests 5 and 6 were made using rectangular configuration W with unequal orifice widths. Unfortunately, experimental difficulties were encountered which invalidated these results. Test 12, however, represents an element configuration analogous to impinging rectangular jets of unequal width. For this case, the oxidizer orifice was rotated 1.570 rad (90 deg) with respect to the fuel orifice. As previously indicated by Fig. 10, a severely distorted spray fan was produced and a loss in η_m of 21.3% was observed.

3. Impingement angle. All tests discussed thus far utilized elements with a 1.047-rad (60-deg) impingement angle. Two additional tests (15 and 16) were made to determine the effect of impingement angle γ on η_m for the rectangular configuration D(MOD) (N_R = 0.54). Although

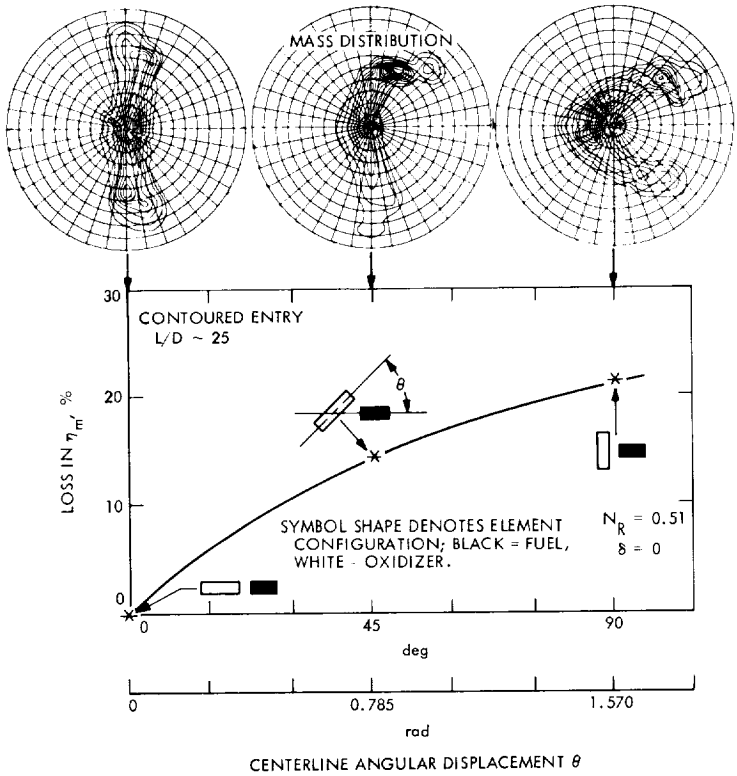

Fig. 10. Mixing efficiency influenced by angular misalignment, rectangular orifice configuration D(MOD)

it is difficult to determine an optimum value on the basis of only three data points, the data of Fig. 11 suggest that an impingement angle of 1.047 rad (60 deg) gives better mixing than either of the other two positions. Tests 17 and 18 also utilized configuration D(MOD) with γ = 1.047 rad (60 deg). Values of N_R of 0.35 and 0.60 produced η_m values of 72.2 and 68.0, respectively. These data are plotted in Fig. 4.

4. Orifice entrance geometry. A primary purpose of determining the mixing characteristics of bipropellant streams using cold flow techniques is to gain confidence that a predictable injector hot firing performance will be achieved (at least on a relative basis, assuming known propellant vaporization rates). If the conditions under which the cold flow data are obtained cause unique hydraulic flow characteristics, the relevance to the hot firing results is questionable.

Several methods are available to the rocket injector designer to provide hydraulic similarity between the cold flow experiments and the hot firing conditions. The most obvious design for promoting freedom from unique flow phenomena such as flip and cavitation is the contoured entry. In a rounded-off opening where the change of direction of streamlines is completed within the orifice length, the area of the jet will then be equal to the orifice area ($C_C \sim 1.0$). Under these conditions, attached, noncavitating streams with negligible radial pressure gradients are formed, and these can subsequently mix in a predictable and reproducible manner. Both the circular and rectangular orifices were evaluated with rounded entrances during this investigation. Both elements yielded mixing results comparable with Rupe's previous data for fully developed impinging circular streams.

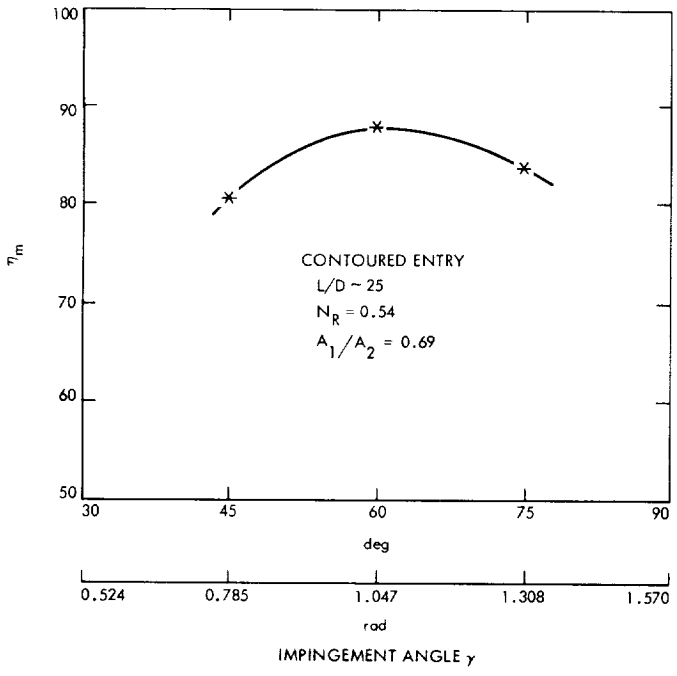

Fig. 11. A correlation of η_m and jet impingement angle for rectangular unlike doublet element, configuration D(MOD)

As previously discussed, configuration A was initially evaluated at JPL with sharp-edged entry. Subsequently, tests 19–22 were run over a range of N_R (0.32–0.65) with rounded inlet orifices, configuration A-RND.

Using orifices with rounded entrances prevented flow separation and therefore cavitation, as shown by JPL data plotted on Fig. 4. These data are shown to be equal to or higher than Rupe's mixing results within acceptable experimental accuracy. The same observations are noted for the previously unpublished results of McHale (Ref. 7), also shown in Fig. 4 for the A-RND element.

E. Summary of Mixing Results

A summary of the mixing results is presented in Fig. 12 for the circular and noncircular orifices. The η_m values have been adjusted to correspond to a 90% collector efficiency so

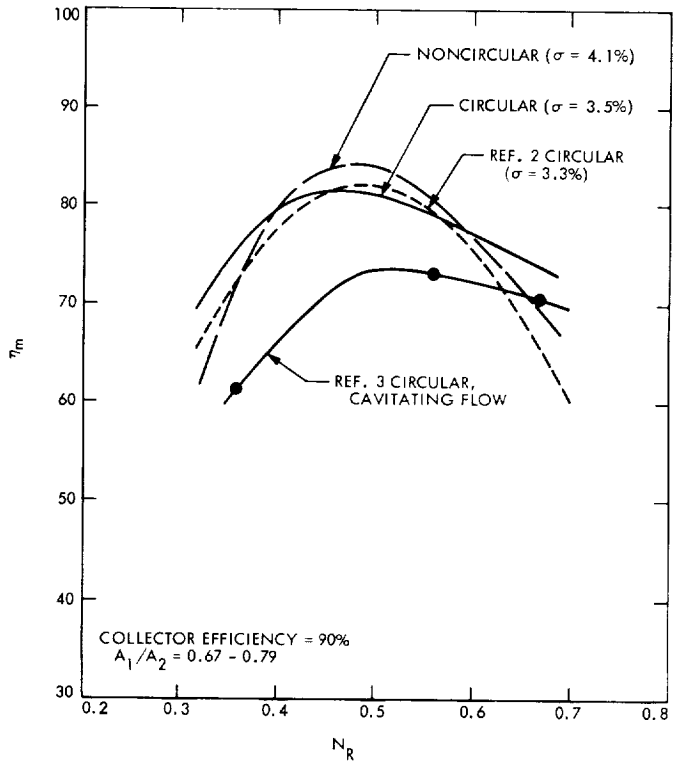

Fig. 12. Summary of mixing results for single-element unlike doublets

that valid comparisons in mixing can be made between data obtained at both agencies.

The lower curve, obtained from Ref. 3, was used by Nurick and McHale to typify their circular orifice data. The data represent liquid phase mixing results obtained with cavitating flow. Orifices that were modified by length and entrance conditions, and/or were subjected to different operating conditions so as to inhibit cavitation, produced η_m values that are commensurate with previously observed mixing levels for circular elements with fully developed turbulent jets.

The noncavitating circular orifices gave a maximum η_m value of 81.5, approximately 8% higher than that for the cavitating flow data of Ref. 3. The higher η_m data agree very closely with the previously published results of Rupe (Ref. 2) for well developed flow from circular jets (η_m = 82.0). The correlating curves represent fourth-degree polynominals and were obtained using a standard statistical regression analysis technique on all the circular noncavitating data shown in Fig. 4 and from particular data of Ref. 2. The standard deviations of the individual data points about their respective estimated correlations were 3.3 and 3.5%, respectively, for the Rupe and current circular orifice mixing results. Similarly, a correlation was established for the noncircular orifice mixing data. As shown in Fig. 12, a maximum η_m value of 84.3 is indicated with a standard deviation of 4.1% obtained for the correlation. Thus, a slight advantage (3.4% increase) is shown for the noncircular orifices, based on the estimated correlating curves. This advantage is not considered significant when the data scatter is considered.

V. Analysis of Results

As indicated above, the JPL data reported herein verify the data of Ref. 3, even to the extent of emphasizing the low values used by Nurick and McHale as a basis of comparison of circular vs noncircular orifices. However, instead of justifying their conclusion, these results and our analysis point out the need to explain the anomalous data obtained for certain sharp-edged-entry circular orifice pairs. The apparent high degree of correlation between "sharp edge" and jet velocity led to a study of the entry conditions in such orifices. The fluid that enters a sharp-edged orifice separates from the boundary at the orifice inlet and a recirculation region is formed. The cross-sectional area of the axially directed core flow at this point is less than the area of the hole. The phenomenon, which is called contraction, is caused by radial pressure gradients just upstream of the orifice inlet. The fluid, as it approaches the orifice, flows radially towards the hole and cannot immediately turn from the radial direction into the direction of the orifice axis. Hall (Ref. 8) refers to this recirculation region as a "separation bubble" and for Reynolds numbers exceeding a certain minimum value, the initially laminar free shear layer bounding the bubble breaks down and reattaches to the orifice wall as a turbulent boundary layer of finite thickness. With sufficiently short orifices and for high flow velocities, this initial separation may cause the core flow to remain detached for the entire length of the orifice.

Ito (Ref. 9) showed that for the vena contracta region, the stream velocity and recirculation velocity profile is also a function of Reynolds number. He further states that the free stream potential flow is decelerated at the outer periphery due to viscous shear drag caused by the semistagnant fluid in the recirculation zone. This causes the jet stream boundary layer to spread until it eventually reattaches to the wall. The velocity deceleration at the free stream boundary results in a mean static pressure recovery. However, even after reattachment is established, fluid cavitation still persists in the entry region, is masked by the downstream flow, and produces flow discontinuities and/or instabilities in the free jet.[5]

Hall relates the effect of orifice fluid cavitation on the discharge flow coefficient C_D of sharp-edged orifices. Northup (Ref. 10) studied the effect of back pressure P_B on the flow stability in small circular orifices; he included entrance geometry, manifold cross velocity, and L/D effects. Nurick and McHale (Ref. 3) extended the study to include noncircular shaped orifices. In addition to visual observations of the free jet appearance, these previous investigators measured orifice C_D values over a range of injection velocities as an indicator of stream stability and operating characteristics. Analytical models have been developed by Riebling and Powell (Ref. 11), and Nurick and McHale, that correlate C_D with orifice design parameters and operating flow conditions.

[5]The term cavitation as discussed herein denotes the sudden transition of a flowing fluid from the liquid to the vapor phase. This change is known to occur whenever the static pressure of the liquid falls below the vapor pressure of the fluid. As the flow through the orifice is increased, the static pressure within the recirculation zone will decrease. If it decreases until it equals the vapor pressure of the liquid P_V, cavitation will occur in the separated region, generating large quantities of vapor which seek an exit. Ito reasoned that cavitation at the vena contracta results in a low recovery rate in the free stream static pressure because the low viscosity vapor in the recirculation zone is capable of sustaining high shear effects with little free-stream deceleration. Expansion and reattachment then cease, the jet flows free of the walls, and $P_T = P_B$ (see Fig. A-1 of Appendix) because of the access of the separated region to the downstream region. Hydraulic flip is then said to have occurred.

The following discussion also concerns the effects of cavitation on orifice flow characteristics and further relates these effects to bipropellant liquid stream mixing.

A. Circular Orifice Cavitation

Cold flow results of C_D vs ΔP for the sharp-edged circular orifices (configuration A) observed for the previously discussed mixing data tests are presented in Fig. 13. The data are plotted separately for each propellant simulant. The upper plot was obtained for the fuel side orifice using water and the lower plot represents the oxidizer side, using trichloroethylene. All data were generated under atmospheric back pressure using the fluids at ambient temperature.

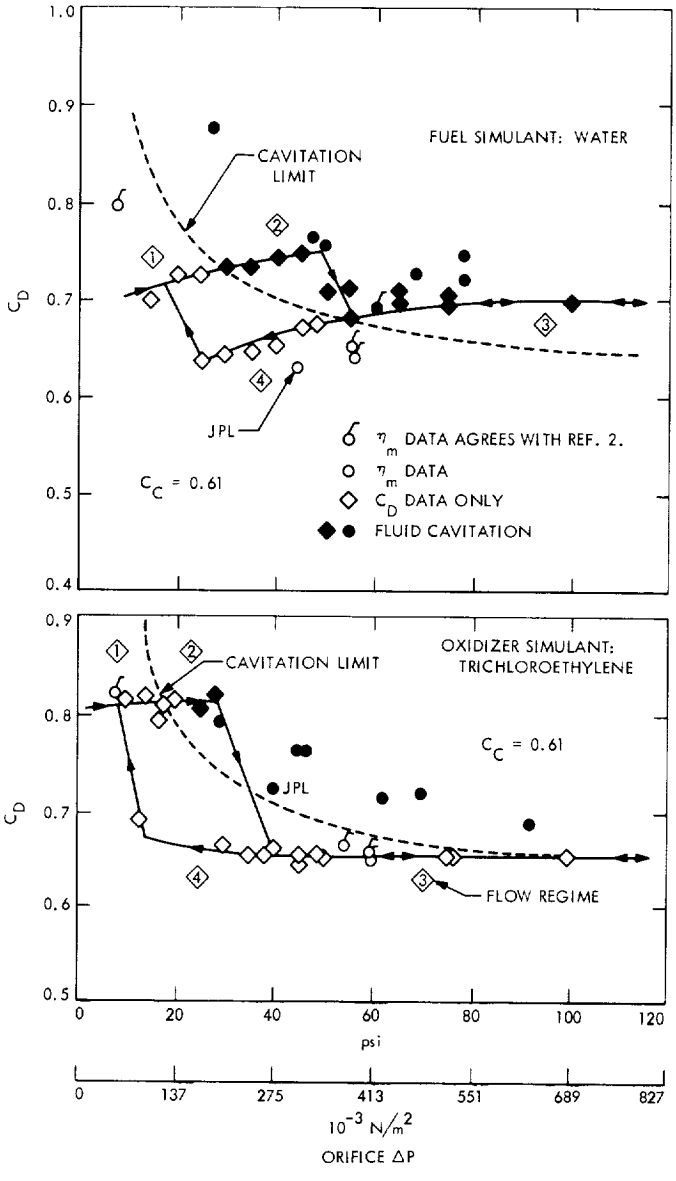

Fig. 13. Correlation of circular orifice flow characteristics with cavitation

Supplementary data were also obtained over a continuous ΔP range with the JPL configuration A element to observe the flow characteristic of the sharp-edged circular orifices. These results are correlated by solid lines in Fig. 13, which pass through various flow regimes. The following visual observations relate the appearance of the jets to the corresponding measurements of C_D and η_m over the ΔP range investigated.

As the water flow was initiated, a circular jet was formed, glassy in appearance, and was attached to the orifice walls at the exit area. This condition is referred to as region ① in the upper part of Fig. 13 and is characterized by a relatively high C_D and η_m. The flow, initially separated at the orifice entrance, had fully reattached, was noncavitating, and is illustrated in Fig. 14. The ΔP was then gradually increased to 199 × 10^3 N/m^2 (29 psi), whereupon the jet exhibited a clouded or gassy appearance. At this flow condition, the static pressure within the separation region at the sharp-edged orifice entry was apparently equal to or less than the water vapor pressure. This cavitating flow regime is identified as region ② in Figs. 13–14 and is characterized by a relatively high C_D (0.7-0.9) with low η_m. During this period, the jet appeared brushy; however, it remained attached to the orifice walls. It is significant to note that even though the measured orifice discharge coefficients were high for this operating condition, the mixing level was lower than that representative of noncavitating flow. As the flow rate was increased, corresponding to a pressure drop of 338 × 10^3 N/m^2 (49 psi), the stream suddenly jumped free of the walls for the entire length of the orifice. A sudden discontinuity in C_D vs ΔP was observed because hydraulic flip had occurred.

Similar flow characteristics were observed for the oxidizer side of the element as shown in the lower part of Fig. 13. However, after flip, the flow regime ③ is shown to exist below the critical cavitation limit. This suggests that the separation cavity has vented to atmospheric back pressure ($P_V = P_B$), causing cavitation to cease.

Visual observations of either stream after hydraulic flip indicate a continual jumping or flickering of the streams at constant ΔP. The streams oscillate erratically within the orifice bore, as illustrated by an actual photograph in Fig. 14 for regime ③. This type of flow instability (intermittent reattachment) was also observed by Northup (Ref. 10) and was amplified by the addition of cross velocity at the orifice entrance. The effect became greater as the ΔP was

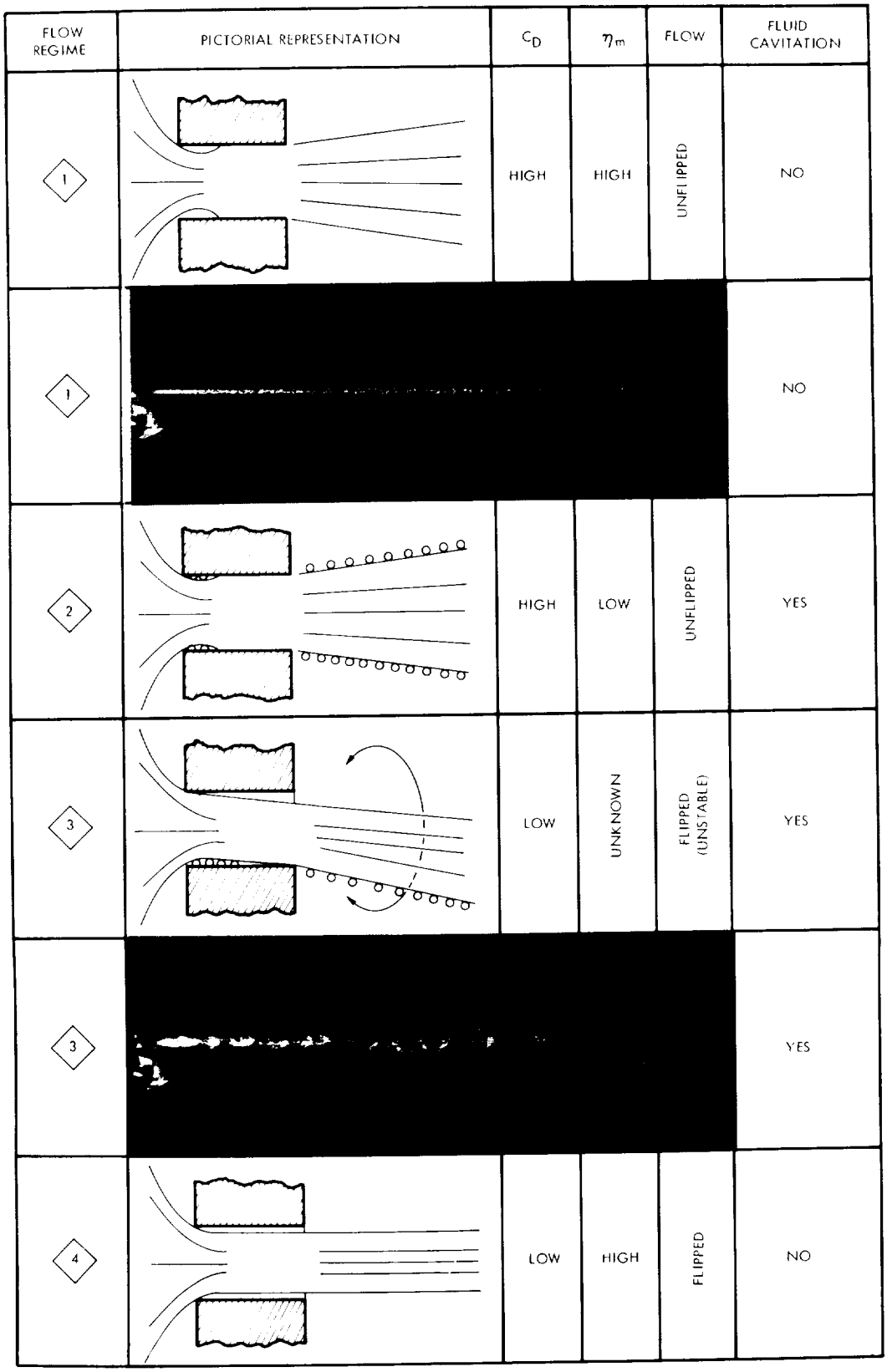

Fig. 14. Sharp-edged circular orifice flow characteristics

increased, resulting in a highly agitated and erratic stream at pressures greater than 414×10^3 N/m^2 (60 psi). Region ③ is characterized by relatively low C_D values (0.6–0.7) and unpredictable stream mixing, depending upon the level of flow instability.

For the fuel side, the instability continued until the water ΔP was reduced to 365×10^3 N/m^2 (53 psi). At that point, all evidence of cavitation and stream instabilities ceased; however, the streams remained in the unattached (flipped) condition, region ④. The jet characteristics now appeared similar to that from a classical sharp-edged orifice. The C_D remaind low, but the stream appearance returned to its original glassy state (void of vapor bubbles) and good mixing efficiencies were again assured. Thus, a condition is now identified whereby the orifice discharge coefficient is low but good stream mixing efficiency is obtained. It is apparent, based upon these data, that to achieve reproducible results and high η_m for circular liquid bipropellant streams, fluid cavitation must be eliminated.

The water jet remained unattached until the ΔP was further lowered to a value of 172×10^3 N/m^2 (25 psi). At that point, the stream reattached to the walls (unflipped) and the initial flow characteristics were again established. It is noted that hydraulic flip that resulted with decreasing flow rate occurred at a lower ΔP, causing a flow-hysteresis phenomenon.

In Fig. 13, the hysteresis loop for both propellants is traversed by a dashed line that represents an analytically derived cavitating limit:

$$(\Delta P)_{\text{critical}} = \frac{P_B - P_V}{\alpha^2 - 1} \cdot \tag{4}$$

The derivation of Eq. (3), first reported by Hall (Ref. 8) in 1963, is given in the Appendix. The expression relates the minimum orifice ΔP to cause fluid cavitation at the vena contracta to the back pressure P_B, fluid vapor pressure P_V, and orifice flow coefficients ($\alpha = C_D/C_C$).

Those cold flow tests that produced ΔP values above the critical value are predicted to be cavitated. Similarly, those tests with a ΔP value below the critical represent noncavitating flow. It is significant to note that the mixing tests predicted in this way to be cavitated also in general produced low η_m values (Fig. 4). The flagged symbols (Fig. 13) represent those mixing tests where η_m is within ±5% of the usual values for circular unlike doublet elements.

B. Noncircular Orifice Cavitation

As previously indicated in Fig. 4, impinging streams from the noncircular shaped orifices mix as efficiently as those from the fully developed circular elements. If one uses the same fluid cavitation criterion ($C_C = 0.61$) as for the circular orifices, the noncircular orifice mixing data are also predicted to be for cavitating flow.[6] Visual observation of streams, however, shows the appearance to be quite different from that of cavitating circular jets used in these experiments.

The flow characteristics of the configuration D rectangular element were investigated over a range of ΔP values and the results are plotted in Fig. 15. One basic difference is noted for the fuel side; the flow did not experience flip but remained unattached over the entire operating range. Different limits for the inception of fluid cavitation are obtained for different assumed C_C and these limits are indicated in Fig. 15 for C_C values from 0.57 to 0.65. Thus, as a study of Fig. 15 will show, even though the noncircular orifice flows were indicated on Fig. 4 to be noncavitating, this is not conclusively proved by the present analysis because actual C_C values were not determined during the tests.

Visual observation of the free streams formed by the rectangular orifices suggests that two small cavitation zones are formed, one adjacent to each short side of the orifice. When this occurs, the rectangular streams exhibit a brushy appearance along only these two sides of the jet. In comparison, the circular streams were totally encompassed by a cavitating fluid boundary. Therefore, the noncircular impinging streams achieve higher η_m values (probably due to better propellant momentum exchange) than the corresponding cavitating jets from circular orifices.

C. Back Pressure Effects

The fluid cavitation tendency within a particular orifice configuration decreases with increasing back pressure as shown previously by Eq. (3) and graphically in Fig. 16. Even with elevated back pressures, of course, the fluid may still cavitate locally for sufficiently high orifice injection

[6] Equation (3) contains a term α, which is defined as C_D/C_C. The contraction coefficient C_C for a gas jet from an infinitely wide vessel with straight walls has been analytically derived by Pai (Ref. 12) to be equal to $\pi/(\pi + 2)$. Pai further states that for a noncircular shape the coefficient of contraction is only slightly different from that of a circular one and since the derivation is generally quite complicated and beyond the scope of this investigation, the numerical value for C_C (0.61) was expected for either shape.

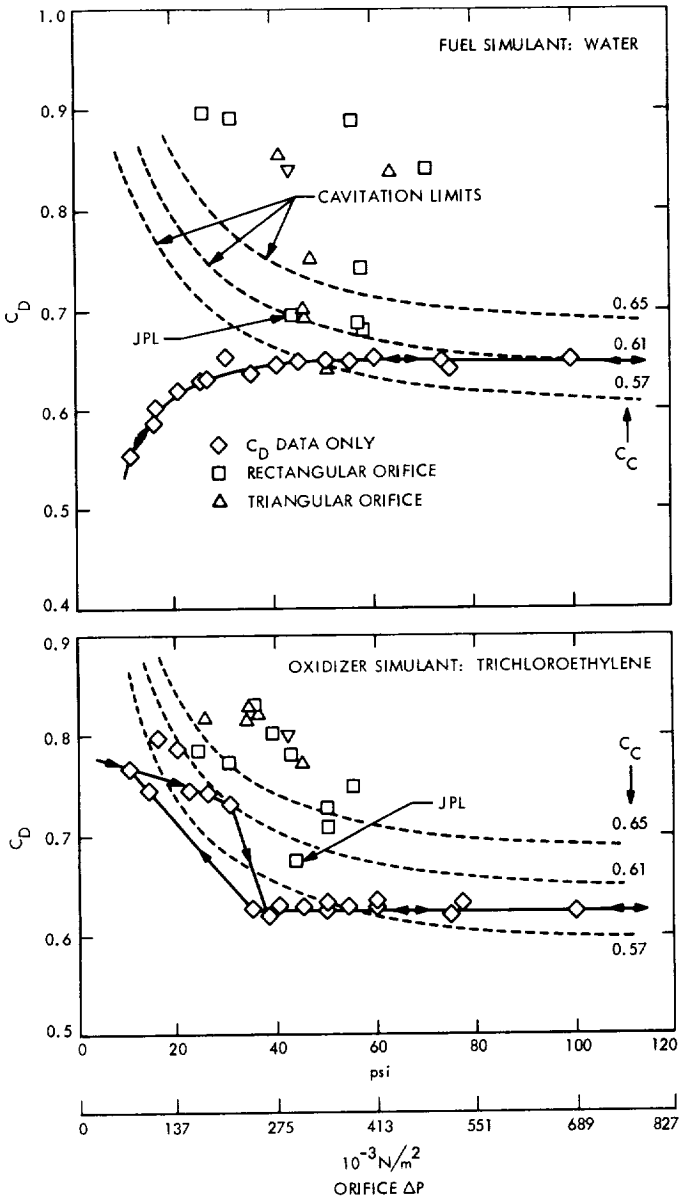

Fig. 15. Correlation of noncircular orifice flow characteristics with cavitation

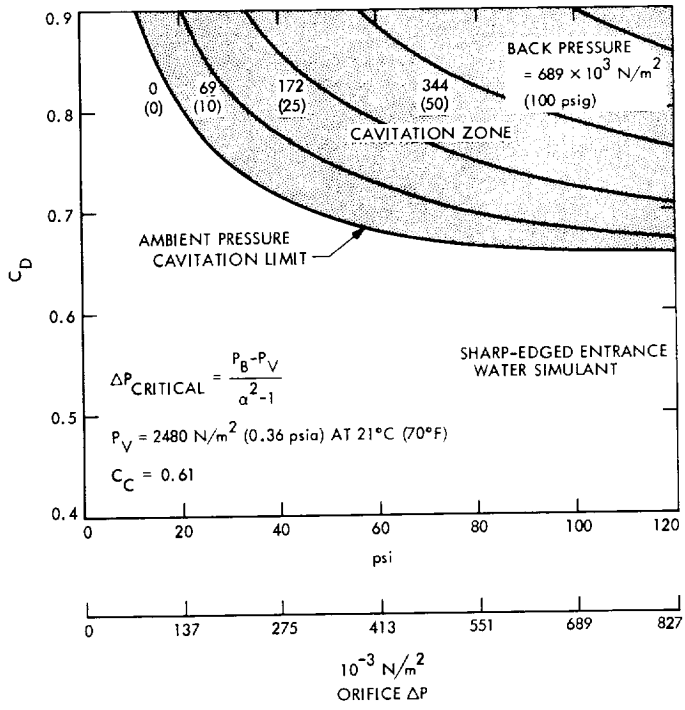

Fig. 16. Effect of back-pressure on circular orifice flow cavitation

velocities. At ambient pressure, cavitation is predicted for all sharp-edged, circular orifices if the C_D and ΔP characteristics fall below the lower limit curve of Fig. 16. Associated with cavitation are hydraulic flip, stream instabilities, and premature jet breakup. Premature jet breakup of circular streams prior to impingement produces sprays that are poorly mixed.

At a back pressure of 344 × 10^3 N/m^2 (50 psig), most practical circular orifice cold flow conditions could be achieved without fluid cavitation. Elevated back pressure, of course, is the typical condition encountered in steady state rocket engine operation.

VI. Summary

Results can be summarized as follows:

(1) The mixing of impinging liquid jets formed by noncircular orifices correlated with stream velocity heads and orifice hydraulic diameter ratios using techniques previously developed for circular unlike doublet elements.

(2) Noncircular elements produced mixing efficiencies similar to those for circular unlike doublets; however, the mixing characteristics can be compared only when the liquid streams have similar hydraulic characteristics. When this similarity was approximated, the noncircular orifice shapes investigated herein produced slightly higher mixing efficiencies compared with the noncavitating circular configurations. The differences are not considered significant, however. The latter data also show good agreement with previously published data for fully developed, bipropellant impinging streams.

(3) Fluid cavitation adversely affected η_m and must be avoided during cold flow experiments. Cavitation

produced unique hydraulic flow characteristics during the subject program. The mixing results thus obtained are not necessarily relevant to predictions of hot firing performance. The orifice flow conditions commensurate with each experimental value of η_m were compared with a predicted critical ΔP limit to produce fluid cavitation. Those tests predicted to have cavitating orifice flow yielded η_m values not consistent with previously published results. The converse is true for those tests, using circular and noncircular elements, without fluid cavitation.

(4) The occurrence of cavitation with circular orifices correlated well with an analytically derived equation predicting fluid cavitation; however, poorer agreement was observed for noncircular orifices. The correlation relates the minimum orifice pressure drop required to initiate cavitation to the system back pressure, the cold flow simulant vapor pressure, and the orifice flow discharge and contraction coefficients. Stream flow instabilities were also visually correlated with cavitation and orifice discharge coefficient measurements. In addition, the influence of cavitation on the characteristic phenomenon of hydraulic flip was observed for the circular and noncircular shaped orifices.

(5) On the basis of limited experimental mixing data, noncircular element stream impingement is shown to be more sensitive to absolute centerline alignment than is stream impingement from corresponding circular jets. The designer of doublets utilizing rectangular orifices must also concern himself with the relative angular orientation of each orifice within the element.

VII. Conclusions

For particular orifice lengths, noncircular shapes were shown to produce more fully developed flows (shorter recovery lengths) and therefore provided several percent higher cold flow mixing uniformities than circular shaped orifices of equal length. However, this mixing disparity cannot necessarily be related to shape alone, nor can it be extrapolated to all noncircular orifice geometry design conditions. Therefore, exception is taken with the original conclusion (Ref. 3) that "Noncircular elements produce *significantly* better mixing than a circular doublet at equivalent design conditions." The conclusion based upon the present data is that the reasons for using noncircular orifices in injectors must stem primarily from considerations other than mixing effectiveness.

Nomenclature

A orifice area

C sample-area correction factor (cross-sectional area of that portion of a sphere that would be represented by the spray sample/cross-sectional area of sample tube)

C_C orifice contraction coefficient, A_T/A

C_D orifice discharge coefficient, actual flow rate/ideal flow rate

D orifice hole diameter

G local mass flux

g gravitational constant

K cavitation number (see Appendix)

L orifice length

N_R correlating parameter for liquid phase mixing (defined in Eq. 2)

n number of samples with $R > r$

$\overline{n}$ number of samples with $R < r$

P pressure

r local mass fraction collected,

$$w_2/(w_1 + w_2) \text{ with } R > r$$

$\overline{r}$ local mass fraction collected,

$$\overline{w}_2/(\overline{w}_1 + \overline{w}_2) \text{ with } R < r$$

R injection mass fraction,

$$W_2/(W_1 + W_2)$$

t sampling period

V axial injection velocity

w local mass of spray collected with $R > r$

$\overline{w}$ local mass of spray collected with $R < r$

$W = \dot{W}t$

$\dot{W}$ total flow rate of injected simulants

x noncircular orifice width

α ratio C_D/C_C

β angle of momentum vector

γ impingement angle

δ orifice centerline displacement

η_c collector efficiency (defined in Eq. 3)

η_m mixing efficiency (defined in Eq. 1)

θ angular position of orifice

ρ liquid density

σ standard deviation of data about estimated correlation

ϕ correlating parameter,

$$\frac{\rho_1 V_1^2 D_1}{\rho_2 V_2^2 D_2}$$

Subscripts

B back

C cross

D discharge

h hydraulic

0 stagnation

T throat

V vapor

1 first component of a spray, i.e., water to simulate fuel

2 second component of a spray, i.e., trichloroethylene to simulate oxidizer

APPENDIX

Derivation of Cavitation Equation (After Hall, Ref. 8)

Consider a square-edged entrance circular orifice supplied with a fluid at pressure P_0 and negligible entrance velocity (Fig. A-1). Due to manifold radial pressure gradients, the liquid flow contracts upon entering, forming a vena contracta of area A_T where the static pressure and uniform axial velocity are P_T and V_T, respectively. Noncavitating flow reattaches to the orifice boundary and exits with velocity V_D to a back pressure P_B. The core flow velocity profile is assumed uniform.

Bernoulli's equation can be written for relatively short orifices in terms of a uniform velocity profile to establish a relationship between the pressure at the vena contracta to the system back pressure:

$$P_0 = P_B + \frac{\rho V_D^2}{2g} = P_T + \frac{\rho V_T^2}{2g} \tag{A-1}$$

$$P_0 - P_B = \frac{\rho V_D^2}{2g} = \Delta P_{\text{measured}}$$

$$C_D \equiv \frac{W_{\text{actual}}}{W_{\text{ideal}}} \text{ by definition of orifice discharge coefficient.} \tag{A-2}$$

From the continuity equation,

$$\frac{W_{\text{actual}}}{\rho} = C_D A V_D = A_T V_T$$

$$V_D C_D = \left(\frac{A_T}{A}\right) V_T = C_C V_T$$

where

$$C_C \equiv \frac{A_T}{A} \tag{A-3}$$

by definition of orifice contraction coefficient.

The combination of Eqs. (A-1) and (A-3) gives

$$P_B - P_T = \frac{\rho}{2g}(V_T^2 - V_D^2) = \frac{\rho}{2g}\left(V_D^2 \frac{C_D^2}{C_C^2} - V_D^2\right) = \frac{\rho V_D^2}{2g}\left(\frac{C_D^2}{C_C^2} - 1\right)$$

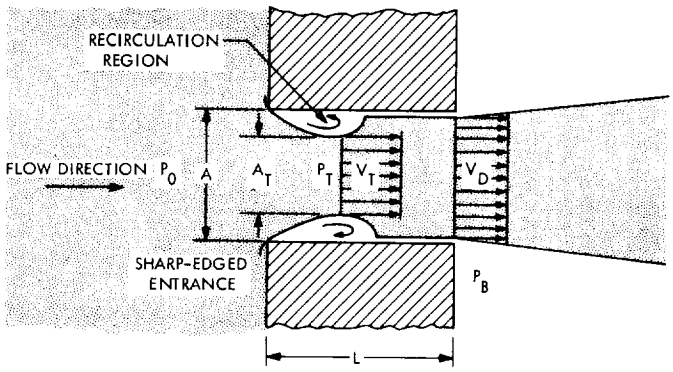

Fig. A-1. Flow through sharp-edged orifice

and

$$\frac{P_B - P_T}{\Delta P_{\text{measured}}} = \frac{C_D^2}{C_C^2} - 1. \tag{A-4}$$

For the special case of cavitation inception,

$$P_T = P_V$$

where P_V = fluid vapor pressure:

$$\frac{P_B - P_V}{\Delta P_{\text{critical}}} = \left(\frac{C_D}{C_C}\right)^2 - 1. \tag{A-5}$$

This equation was first derived by Hall (Ref. 8) in 1963. It is similar to the expression relating stream cavitation to flow around a streamlined solid body immersed in a fluid. For a body of given shape and orientation, the criterion for avoiding local cavitation is to maintain a cavitation number $K > (\alpha^2 - 1)$, where α is a dimensionless constant dependent only on the bubble shape (Ref. 13). For sharp-edged orifice flow, the value for α becomes

$$\frac{C_D}{C_C}.$$

The critical ΔP necessary to cause fluid cavitation at the vena contracta of a sharp-edged orifice can be written

$$\Delta P_{\text{critical}} = \frac{P_B - P_V}{\alpha^2 - 1}. \tag{A-6}$$

References

1. Rupe, J. H., *The Liquid-Phase Mixing of a Pair of Impinging Streams*, Progress Report 20-195. Jet Propulsion Laboratory, Pasadena, Calif., Aug. 6, 1953.

2. Rupe, J. H., *A Correlation Between the Dynamic Properties of a Pair of Impinging Streams and the Uniformity of Mixture-Ratio Distribution in the Resulting Spray*, Progress Report No. 20-209. Jet Propulsion Laboratory, Pasadena, Calif., Mar. 28, 1956.

3. Nurick, W. H., and McHale, R. M., *Noncircular Orifice Holes and Advanced Fabrication Techniques for Liquid Rocket Injectors*, Phase I Final Report, NASA CR-108570. Rocketdyne Division of North American Rockwell Corp., Oct. 1970.

4. Johnson, B., *An Experimental Investigation of the Effects of Combustion on the Mixing of Highly Reactive Liquid Propellants*, Technical Report 32-689. Jet Propulsion Laboratory, Pasadena, Calif., July 15, 1965.

5. Houseman, J., "Optimum Mixing of Hypergolic Propellants in an Unlike Doublet Injector Element," *AIAA J.* Vol. 8, No. 3, pp. 597–599, Mar. 1970.

6. Gerbracht, F. G., "Injector Hydraulics," in *Supporting Research and Advanced Development*, Space Programs Summary 37-47, Vol. III, pp. 149–153. Jet Propulsion Laboratory, Pasadena, Calif., Oct. 31, 1967.

7. McHale, R. M., Rocketdyne Division of North American Rockwell Corp., private communication.

8. Hall, G. W., "Analytical Determination of the Discharge Characteristics of Cylindrical-Tube Orifices," *J. Mech. Eng. Sci.*, Vol. 5 No. 1, pp. 91–97, 1963.

9. Ito, J. I., "A General Model Describing Hydraulic Flip in Sharp Edge Orifices," in *7th JANNAF Combustion Meeting*, CPIA Publication 204, Vol. I, pp. 417–426. Chemical Propulsion Information Agency, The Johns Hopkins University, Silver Spring, Md., 1971.

10. Northup, R. P., "Flow Stability in Small Orifices," Paper presented to American Rocket Society in Atlantic City, N. J., Nov. 30, 1951.

11. Riebling, R. W., and Powell, W. B., "The Hydraulic Characteristics of Flow through Miniature Slot Orifices," Technical Report 32-1397. Jet Propulsion Laboratory, Pasadena, Calif., Sept. 15, 1969.

12. Pai, Shih-I, *Fluid Dynamics of Jets*, D. Van Nostrand Company, Inc., New York, 1954.

13. Batchelor, G. K., *An Introduction to Fluid Dynamics*, Cambridge University Press, Great Britain, 1967.

NASA — JPL — Coml., L.A., Calif.